Atlas-Based Under-Segmentation

Christian Wachinger[1,2], Polina Golland[1]

[1]Computer Science and Artificial Intelligence Lab (CSAIL), MIT

[2]Massachusetts General Hospital, Harvard Medical School

Introduction

- Atlas-based segmentation is commonly used in medical image analysis
- Tendency of atlas-based segmentation to under-segment structures
- Dice overlap and Hausdorff distance do not measure under-segmentation
- Wang, Yushkevich (2012) proposed deconvolution of label maps
- Contributions:
  - Volume overlap measures to quantify under-segmentation
  - **Hypothesis: asymmetry in single organ segmentation as cause**
  - Generative model of background to correct under-segmentation

Segmentation of parotid glands in CT images

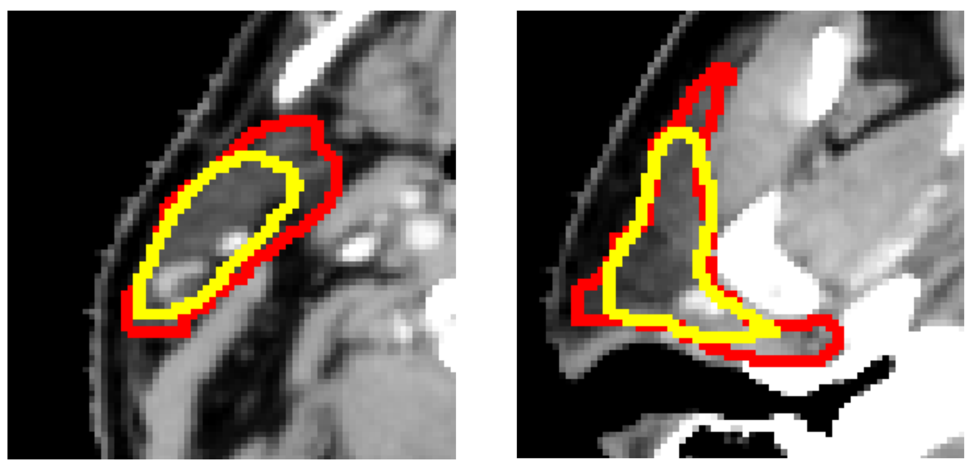

Red: manual, Yellow: automatic

Merging several structures to one background label

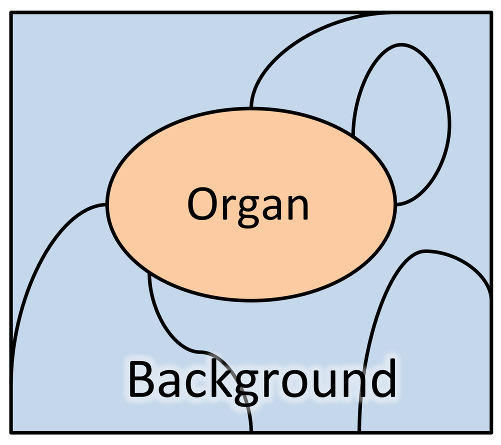

Under-Segmentation

Measures to quantify over- and under-segmentation:

$$O(\hat{S}, \bar{S}) = \frac{|\hat{S} \setminus \bar{S}|}{|\bar{S}|} \qquad U(\hat{S}, \bar{S}) = \frac{|\bar{S} \setminus \hat{S}|}{|\bar{S}|}$$

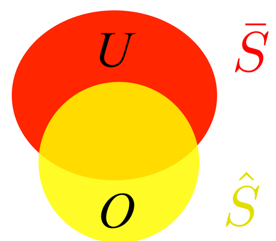

$\bar{S}$: Manual $\hat{S}$: Automatic segmentation

- Quantitative segmentation results for three applications
- Under-segmentation errors significantly higher than over-segmentation errors

Left atrium in heart MRA

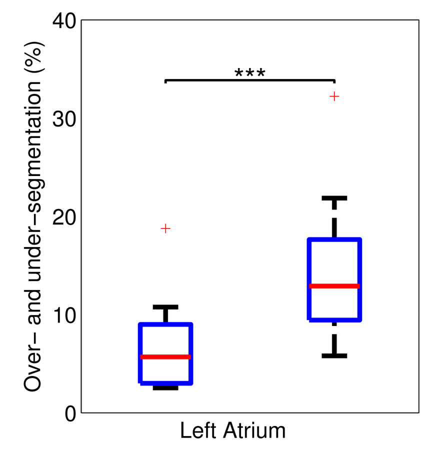

Parotid glands in head & neck CT

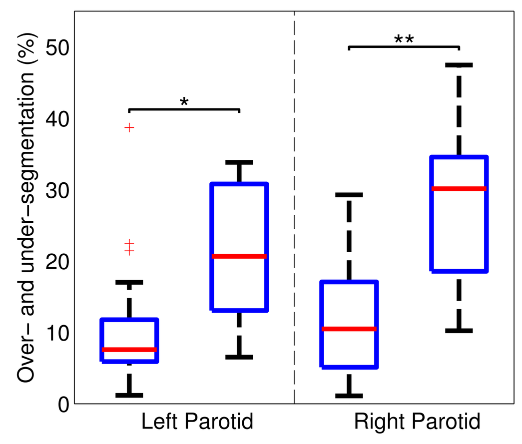

First column: over-segmentation
Second column: under-segmentation

Nine brain structures in MRI
Foreground-background segmentation

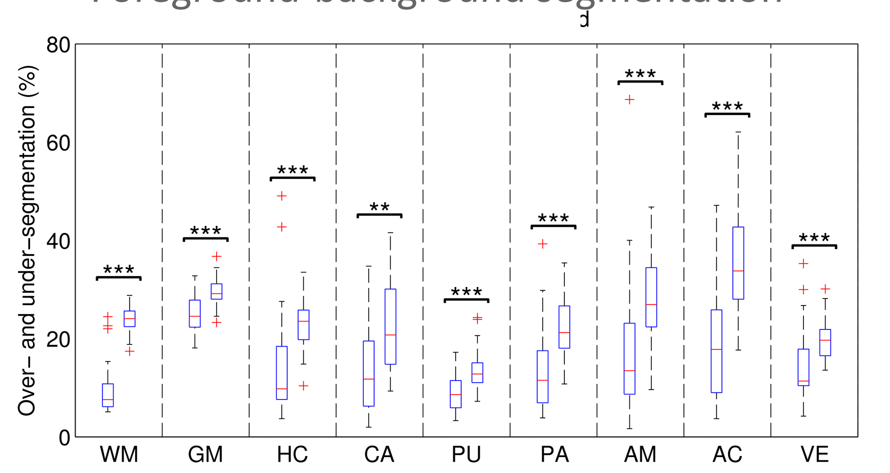

White matter (WM), Gray matter (GM), Hippocampus (HC), Caudate (CA), Putamen (PU), Pallidum (PA), Amygdala (AM), Accumbens (AC), Ventricles (VE)

Hypothesis for under-segmentation

- Under-segmentation is caused by asymmetry in foreground-background segmentation
- Merging all surrounding labels into background creates a new meta-label that dominates the voting process
- Multi-organ segmentation of brain supports hypothesis

Illustration of multi-organ and foreground-background segmentation

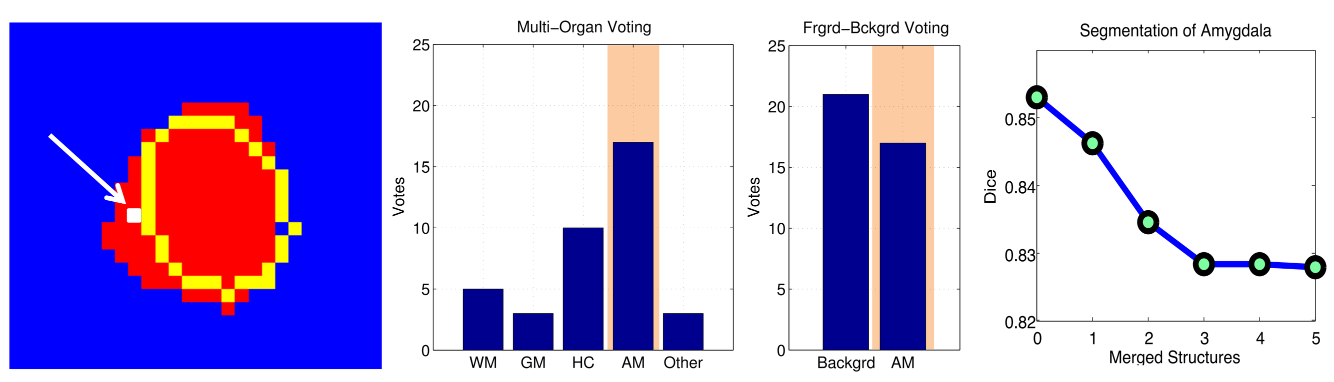

Red: manual, Yellow: automatic, White: voxel of interest

Multi-organ brain segmentation

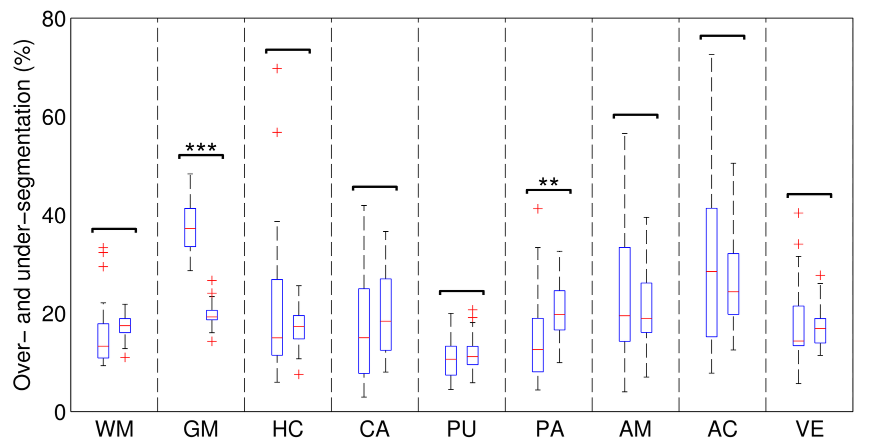

Latent multi-label model of the background

- Generative model for the unsupervised separation of the background in *K* components and simultaneous estimation of *K*
- Dirichlet process Gaussian mixture model (DP-GMM) on patches:

$$\mathcal{P} = \{P_{ix} : x \in \Gamma, S_i(x) = b\}$$

- Replace background label with mixture component:

$$S_i(x) = b \quad \Rightarrow \quad S_i(x) = z_{ix} \qquad z_{ix} \in \{1, \ldots, K\}$$

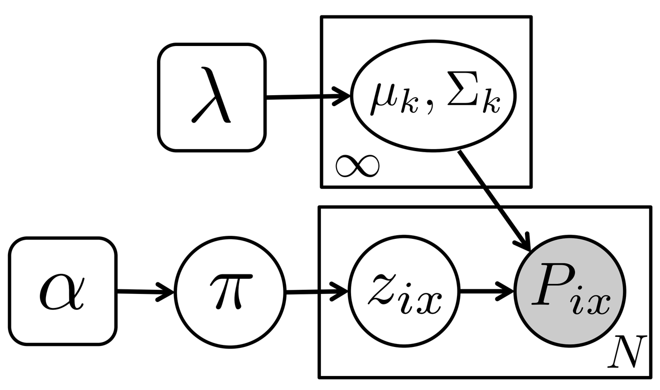

$$P_{ix} | z_{ix} \sim \mathcal{N}(\mu_{z_{ix}} \Sigma_{z_{ix}})$$
$$z_{ix} \sim \mathrm{Cat}(\pi)$$
$$\pi \sim \mathrm{GEM}(\alpha)$$
$$(\mu_k, \Sigma_k) \sim \mathcal{NW}(\lambda)$$

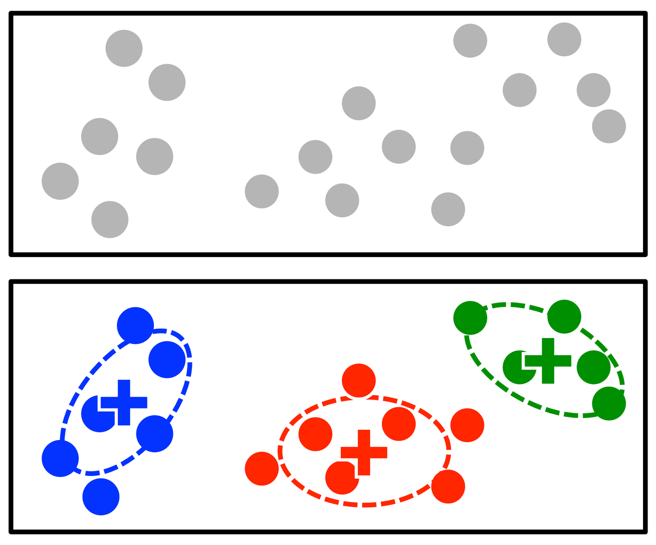

Multi-atlas segmentation

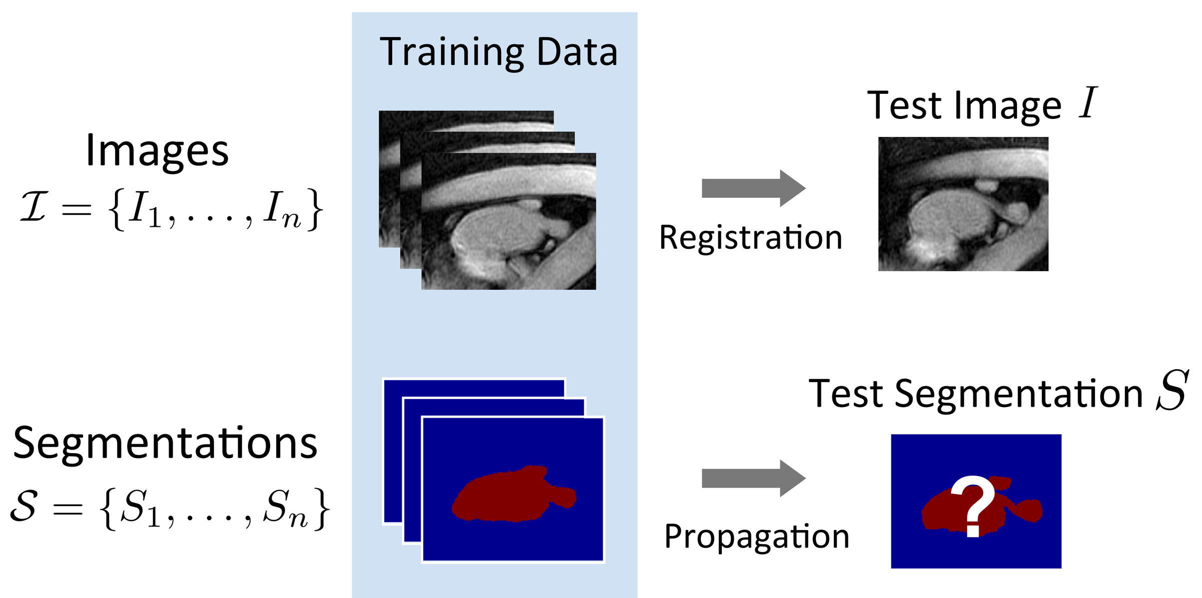

Label maps specify likelihood of each label:

$$L^l(x) = \sum_{i=1}^{n} p(S(x) = l | S_i) \cdot p(I(x) | I_i) \qquad l \in \{1, \ldots, \eta\}$$

Label likelihood term:

$$p(S(x) = l | S_i) = \begin{cases} 1 & \text{if } S_i(\phi_i(x)) = l, \\ 0 & \text{otherwise.} \end{cases}$$

Intensity likelihood term:

$$p(I(x) | I_i) \propto \exp\left(-(I(x) - I_i(\phi_i(x)))^2 / 2\sigma^2\right)$$

Most likely label yields segmentation:

$$\hat{S}(x) = \arg\max_l L^l(x)$$

Foreground-Background segmentation:

$$L^f(x) > L^b(x)$$

Results

- Datasets:
  - 16 heart MRA images (0.6x0.6x1.5mm)
  - 18 head and neck CT scans (0.9x0.9x2.5mm)
  - 39 brain MRI with 1mm isotropic resolution
- Comparison to deconvolution (Wang, 2012)
- Details:
  - DP-GMM, GMM, DP-means, k-means
  - Global and local approach
  - Patch size: 3 x 3 x 3

Left Atrium

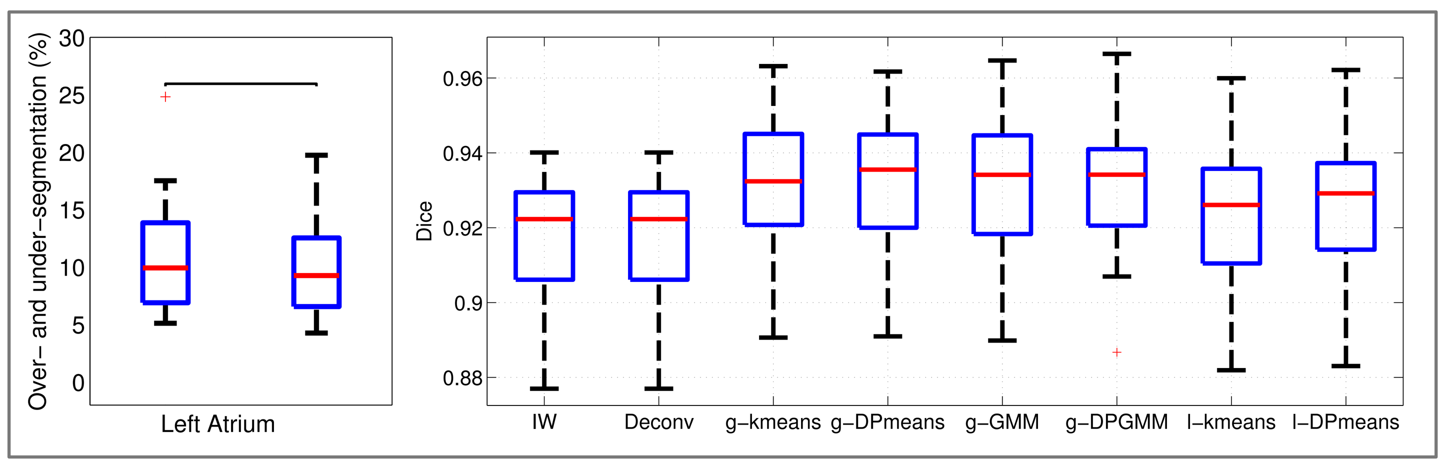

Brain

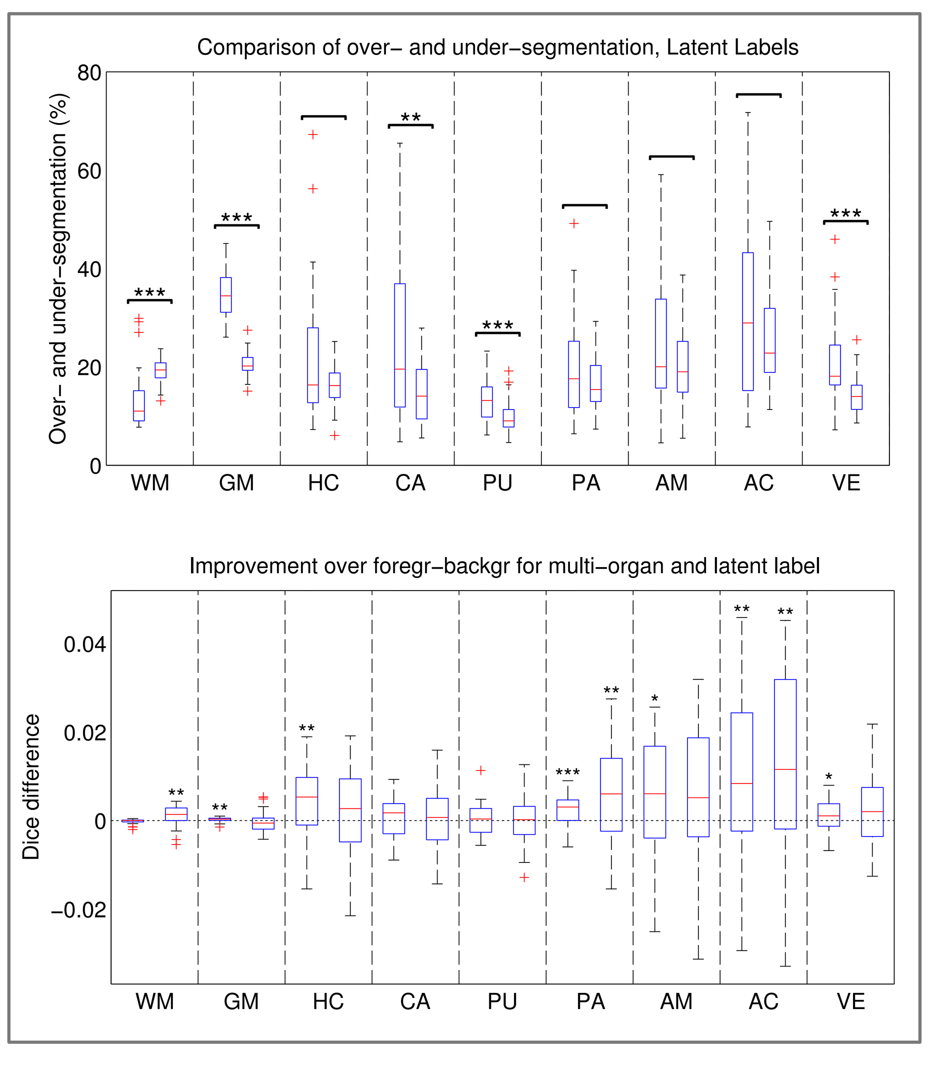

Parotid Glands

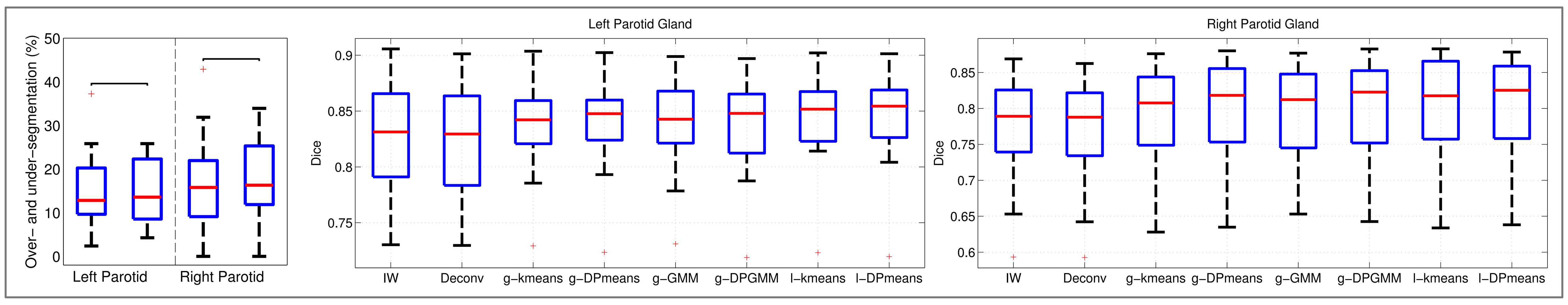

Conclusions

- Significant bias in atlas-based segmentation to under-segmentation
- Asymmetry in foreground-background segmentation as new hypothesis
- Generative model to partition background reduces under-segmentation

Acknowledgement:
We thank Jason Chang and Greg Sharp. This work was supported in part by the National Alliance for Medical Image Computing (U54-EB005149) and the NeuroImaging Analysis Center (P41-EB015902).